

**Stellar Population of Ellipticals in Different Environments:  
Near-infrared Spectroscopic Observations**

**P. A. James<sup>1</sup> and B. Mobasher<sup>2</sup>**

<sup>1</sup> Astrophysics Research Institute, Liverpool John Moores University,  
Twelve Quays House, Egerton Wharf, Birkenhead L41 1LD.

<sup>2</sup> Astrophysics Group, Blackett Laboratory, Imperial College,  
Prince Consort Road, London SW7 2BZ.

*Accepted for publication in the Monthly Notices of the Royal Astronomical Society*

**ABSTRACT**

Near-infrared spectra of 50 elliptical galaxies in the Pisces, A2199 & A2634 clusters, and in the general field, have been obtained. The strength of the CO ( $2.3 \mu\text{m}$ ) absorption feature in these galaxies is used to explore the presence of an intermediate-age population (e.g. Asymptotic Giant Branch stars) in ellipticals in different environments. We find the strongest evidence for such a population comes from ellipticals in groups of a few members, which we interpret as the result of recent minor merging of these galaxies with later type galaxies. Field galaxies from very isolated environments, on the other hand, show no evidence for young or intermediate-age stars as revealed by  $\text{H}\beta$  and CO absorptions, and appear to form a very uniform, old population with very little scatter in metallicity and star formation history.

**Key words:** galaxies: clusters - galaxies: elliptical - galaxies: fundamental parameters - galaxies: stellar content - infrared: galaxies.

## 1 INTRODUCTION

Elliptical galaxies are conventionally assumed to have stellar populations dominated by old stars, formed in a single burst some 12–16 Gyr ago. However, the degree to which this assumption is violated in observed systems is very uncertain. Indeed, some of the studies regarded as underpinning this view express distinct reservations on the accuracy of this picture. For example, Tinsley & Gunn (1976) point out that their modelling of optical and near-infrared colour and line indices of ellipticals cannot rule out the existence of ‘a considerable population of stars born after the rapid initial burst’ (see also Bruzual 1983). However, more recent studies show that less than 10 per cent of the stars in present-day ellipticals are likely to have been formed in the last 5 Gyr, imposing strong constraints on the time and duration of the last episode of star formation in ellipticals (Bower, Lucey & Ellis 1992). Moreover, using UV-optical colours of ellipticals in clusters at  $z \simeq 0.5$ , Ellis et al. (1997) confirm that star formation in most cluster ellipticals was essentially completed by  $z \simeq 3$ .

However, one outstanding question is whether field ellipticals, which are currently isolated or surrounded by at most a small number of neighbours, have the same star formation history as their cluster counterparts. Indeed, several observational studies have found strong evidence that they do not, with the star formation extending to significantly more recent times in the case of field ellipticals. For example, Larson, Tinsley & Caldwell (1980) found that bright field ellipticals are, on average, bluer than cluster ellipticals of the same luminosity, implying more recent star formation in the former. Furthermore, O’Connell (1980) showed that major star formation episodes in the nearby blue elliptical M 32 continued until  $\sim 5$  Gyr ago while, using optical spectroscopy, Bica & Alloin (1987) concluded that field ellipticals and lenticulars contain an intermediate-age component, not present in cluster ellipticals. These results were further confirmed by Bower et al. (1990) and Rose et al. (1994) who used a range of optical spectral indicators to infer that ‘a substantial intermediate-age population is present in the early-type galaxies in low-density environments, a population that is considerably reduced or altogether lacking in the early-type galaxies in dense clusters’. Similarly, Schweizer & Seitzer (1992) found that some field ellipticals have blue UV-optical colours and strong  $H\beta$  absorption lines, indicating star formation within the last 3–5 Gyr. Also, the range in  $H\beta$  strength observed in field ellipticals was interpreted by Gonzalez (1993) as evidence for an inhomogeneous stellar population. Finally, Kauffmann (1996) showed via simulations of the star formation and merging history of galaxies that star formation can naturally be expected to continue to more recent epochs in low-density environments. An implication of these results, explored by de Carvalho & Djorgovski (1992) and Guzmán & Lucey (1993), is that the younger stellar populations in ellipticals in low-density environments results in an increase in scatter about, and offsets from, the Fundamental Plane of elliptical galaxies (Dressler et al. 1987, Djorgovski & Davis 1987). This has strong implications regarding formation of ellipticals and determination of galaxy distances using the Fundamental Plane.

However, there has recently been an important dissenting opinion, in the work of Silva & Bothun (1998), who study the near-IR colours of a sample of field elliptical galaxies with signs of recent disturbance (i.e. possible post-mergers). They concluded that <10–15 per cent of the stellar mass in these systems is in the form of intermediate-age stars, with ages 1–3 Gyr. The fraction of light contributed by such a population can be somewhat larger, but is still <20–30 per cent. This is a surprising result, because this sample contains just those field galaxies which would be expected to show the strongest signatures of recent star formation.

To address these questions, we carried out a spectroscopic study of elliptical galaxies in different environments, using near-infrared measurements of the  $2.3 \mu\text{m}$  CO 2–0 photospheric absorption feature to determine the contribution from the intermediate-age stellar population to the light

of these galaxies (Mobasher & James 1996; henceforth paper I). We found marginally-significant evidence for deeper CO absorptions, and hence larger intermediate-age populations, in the field galaxies. However, the small sample size (9 field and 12 cluster galaxies) limits the statistical significance of these results. The present paper extends the sample to 50 ellipticals in total (20 field and 30 cluster) and looks in more detail at optimal techniques for extracting information on stellar populations from CO measurements. The near-IR spectral data presented here are for ellipticals in the Abell 2199 and Abell 2634 clusters, and for field galaxies from Faber et al. (1989).

Recent observations and data reduction are outlined in section 2. Section 3 presents results regarding the correlation between star formation history and environment. Section 4 explores the dependence of CO index on the physical parameters in galaxies and discusses some of the relevant peculiarities of individual galaxies. Section 5 contains a comparison of these results with previous studies, and section 6 summarises the main conclusions.

A Hubble constant of  $75 \text{ km s}^{-1} \text{ Mpc}^{-1}$  is assumed in this paper.

## 2 OBSERVATIONS AND DATA REDUCTION

The observations presented here were carried out using the United Kingdom Infrared Telescope (UKIRT) on the 4 nights 1996 August 2–5. The instrument used was the long-slit near-IR spectrometer CGS4, with the  $150 \text{ line mm}^{-1}$  grating and the short-focal-length (150 mm) camera. The 2-pixel-wide slit was chosen, corresponding to a projected width on the sky of 2.4 arcsec. The wavelength range in this configuration in first order was  $0.33 \mu\text{m}$ , centred on the start of the CO absorption band at  $\sim 2.33 \mu\text{m}$  for galaxies with recession velocities of a few thousand  $\text{km s}^{-1}$  (the present sample has redshifts from 1500–12000  $\text{km s}^{-1}$ ). The effective resolution, including the effective degradation caused by the wide slit, was about 900, and the array was moved by 1 pixel between integrations to enable bad pixel replacement in the final spectra.

For each observation, the galaxy was centred in the slit by maximising the IR signal, using an automatic peak-up facility. Total integration times were between 40 minutes and an hour per galaxy, depending on their central surface brightness. During this time, the galaxy was slid up and down the slit at one minute intervals by 22 arcsec, giving two offset spectra which were subtracted to remove most of the sky emission. Stars of spectral types A0–A6, suitable for monitoring telluric absorption, were observed in the same way before and after each galaxy, with airmasses matching those of the galaxy observations as closely as possible (root-mean-square difference  $< 0.1 \text{ A.M.}$ ). Flat fields and argon arc spectra were taken using the CGS4 calibration lamps.

The spectra were reduced using the FIGARO package in the Starlink environment, as outlined in paper I. However, there was an initial complication, resulting from the CGS4 slit rotation mechanism having jammed at the time that these observations were made. This resulted in the slit being substantially misaligned with the columns of the array, which made sky-line subtraction and spectral extraction difficult. The problem was overcome by using the FIGARO routine SDIST to fit the orientations of arc lines in spectra taken during each of the 4 nights. This resulted in a correction which was applied to each spectrum taken using the CDIST routine. This worked very successfully, which was demonstrated by applying the correction obtained from one arc spectrum to another taken on the same night. Arc lines in the corrected spectra were perfectly aligned with the array columns, and the only side-effect was a slight loss of wavelength range as the ends of the corrected spectra subsequently had to be trimmed. This had no impact on the present programme, since the available wavelength range was in excess of that needed. The galaxy flux was then extracted from  $\sim 5$  pixels (i.e. 6 arcsec.) along the slit.

The result of the data reduction was a one-dimensional, wavelength-calibrated galaxy spectrum, which had been divided by an A-star spectrum to remove the effects of atmospheric absorptions. This was converted into a normalised, rectified spectrum by fitting a power-law to featureless sections of the continuum, and dividing the whole spectrum by this power-law, extrapolated over the full wavelength range (see Doyon, Joseph & Wright 1994 for a discussion of this procedure). This fitting process made use of code kindly written by Dr C. Davenhall under the Starlink QUICK facility. The resulting rectified spectrum then has a flat continuum level of unity across the whole wavelength range, simplifying the calculation of equivalent widths and spectral indices of the spectral features. The spectra were wavelength calibrated using the argon arc spectra, and redshift-corrected on the basis of their catalogued recession velocities.

To quantify the depth of the 2.3  $\mu\text{m}$  CO absorption features, several different methods have been proposed. For example, Doyon et al. (1994) use a spectroscopic CO index, defined by

$$CO_{sp} = -2.5 \log \langle R_{2.36} \rangle$$

where  $\langle R_{2.36} \rangle$  is the average value of the rectified spectrum between 2.31 and 2.4  $\mu\text{m}$  in the galaxy rest frame. Doyon et al. (1994) give conversions between this index and the photometric CO index used by earlier studies based on narrow-band filter observations, and also calibrate the index against effective temperature for dwarf, giant and supergiant stars. This was the definition we used to quantify CO depth in paper I. However, Puxley, Doyon & Ward (1997; PDW) have recently proposed a new definition, which they claim to be the most powerful discriminant between different stellar populations in galaxies. Considering various options, they conclude that the optimal wavelength range is 2.2931–2.32  $\mu\text{m}$ , a substantially narrower range than for  $CO_{sp}$ , and they express this as an equivalent width in nm, rather than as an index in magnitudes. Whilst they adopt this measure for astrophysical reasons, there are practical advantages resulting from the narrower wavelength range. Errors resulting from the uncertainty in the power-law fit to the continuum are substantially reduced, because the degree of extrapolation needed is much smaller. Also, the new definition enables higher-redshift objects to be observed without the spectra becoming unduly noisy as the bandpass of interest moves to the end of the K window. On the Mauna Kea site, the window is typically usable to about 2.5  $\mu\text{m}$ , which corresponds to a limit of only 12,500  $\text{km s}^{-1}$  in recession velocity before the end of the  $CO_{sp}$  range is lost, compared to 23,000  $\text{km s}^{-1}$  for the range advocated by PDW.

However, there are arguments against going to the still shorter wavelength range used by, for example, Kleinmann & Hall (1986) and Origlia, Moorwood & Oliva (1993). Their EW measurements were found to be sensitive to velocity-dispersion smoothing, whereas the PDW find their EW to be completely unaffected (we apply no velocity dispersion corrections to the EW in the present paper). In addition, shorter baselines result in reduced signal-to-noise, which would be a significant problem for the fainter galaxies here. Thus, we calculate both the CO EW defined by PDW, and the  $CO_{sp}$  index for comparison with paper I and the calibrations of Doyon et al. (1994). Whilst the prescription given by Doyon et al. (1994) and PDW are simple and, it is to be hoped, unambiguous, the resulting indices and equivalent widths should be regarded as instrumental measures. It would be useful to obtain repeat measurements of the present sample with other telescopes and instruments to check for possible systematic differences, but this has not yet been done.

In calculating the errors in the CO estimates, a number of random and systematic sources of error were taken into account. Random errors consist of both photon counting statistics and weak unresolved spectral features, which effectively introduce similar errors. These were estimated from the standard deviation of the ‘featureless’ continuum used in the power-law fitting, after division by the power-law. This constitutes the dominant error in the CO EW values, due to the

relatively small spectral range on the CO bandhead, whilst the random error on the continuum determination is small because most of the continuum between 2.15 and 2.28  $\mu\text{m}$  can be used. This gives a  $1\text{-}\sigma$  error on the CO EW estimated at 0.2 nm. Determination of the continuum slope from the power-law fitting also contributes to the error, and was estimated by varying the wavelength ranges used in the power-law fitting, and by using different packages and algorithms for the fitting, with errors of 0.2 nm allocated to this cause. Finally, errors due to wavelength calibration and redshift uncertainty were estimated by shifting the spectral bandpass by an amount equivalent to  $\pm 400 \text{ km s}^{-1}$ , and an error of 0.1 nm allocated to this for all measurements. Adding these three sources of error in quadrature, since they are most plausibly uncorrelated with one another, overall errors of 0.3 nm were assigned to the CO EW values.

The CO measurements for the sample of 29 elliptical galaxies in this study (both in field and clusters) are listed in Table 1. This also contains the 21 galaxies from paper I for which new CO measurements have been determined following the prescription of PDW. Column 1 gives the galaxy name. For the cluster galaxies without NGC, UGC or IC numbers, the designator given is either from Butcher & Oemler (1985) or Lucey et al. (1997), and these galaxies are listed in the format  $BOnnn$  or  $Lnnn$  respectively. Column 2 gives the heliocentric recession velocity in  $\text{km s}^{-1}$ , column 3  $CO_{sp}$ , and column 4 the CO EW as defined by PDW, in nm. Column 5 gives the  $H\beta$  equivalent width from Trager et al. (1998), in units of 0.1 nm. Column 6 gives the total B-band absolute magnitude, calculated from  $B_T$  values in the NASA/IPAC Extragalactic Database (NED) and the heliocentric redshift. Column 7 gives the log of velocity dispersion in  $\text{km s}^{-1}$  and column 8 the  $M_{g_2}$  index in magnitudes, both of which were taken from Faber et al. (1989) or Lucey et al. (1997). Column 9 gives the cluster or group membership where HG and GH denote groups from Huchra & Geller (1982) and Geller & Huchra (1983) respectively, and ‘Isol’ denotes galaxies which pass our isolation criterion, which we describe in section 3.

As a check on the overall validity of our data and reduction methods, we calculated the stellar type of stars giving rise to the near-IR light in these galaxies. This involved converting the CO EW values to  $CO_{sp}$  using the equation given by PDW, then using the  $CO_{sp}$ -effective temperature calibration given by Doyon et al. (1994), and finally the effective temperature-spectral type conversion from Allen (1976). We find that the CO absorption strengths for most galaxies are consistent with those of K giants, with a range equivalent to stars of spectral types K3III–K8III. Photometric studies (e.g. Frogel et al. 1978) tend to show that the near-IR light of galaxies is equivalent to that of late K or early M giants, reasonably consistent with our findings.

### 3 ENVIRONMENTAL DEPENDENCE OF CO DEPTH

The distribution of CO EWs for the 50 elliptical galaxies in this study is shown in Fig. 1, where the cluster and field galaxy distributions are shown by solid and dashed lines respectively. The field galaxy distribution is also shaded for clarity. The field galaxies appear to cover a broader range of CO EWs compared to their counterparts in clusters. The field ellipticals also show a pronounced bimodal distribution. Overall, the mean CO strengths for the field and cluster galaxies are similar, corresponding to  $3.28 \pm 0.12$  nm and  $3.29 \pm 0.06$  nm respectively, with the errors being the standard deviations from the mean. However, the apparent difference in the distributions is moderately significant, with a K-S test determining that there is only an 8 per cent chance that the two distributions were drawn from the same parent population. In paper I, the field galaxy distribution was simply displaced towards stronger CO indices (or larger EW values) compared with that for clusters.

However, there is a potential problem, in that the two peaks found in the CO EW distribution

for field galaxies correlate strongly, though not perfectly, with the observing run (there is no such correlation for cluster galaxies). This is in the sense that most of the galaxies in the high EW peak centred on  $\sim 3.8$  nm were observed in the 1994 run described in paper I, whereas the peak centred on 2.7 nm is comprised of galaxies observed in the 1996 run. The difference is significant, with the field galaxies in the 1994 run having a mean CO EW of  $3.82 \pm 0.06$  nm, whereas those observed in the 1996 run have a mean of  $2.88 \pm 0.09$  nm. This immediately raises the question of whether the offset is a systematic, due to some change in the instrument or the data reduction procedures. We take this possibility extremely seriously, and in the following discussion examine all the possibilities to explore the reality of this effect. We emphasize here that the CO EW values for the cluster galaxies observed in 1994 had an average value of  $3.34 \pm 0.09$  nm, compared with  $3.25 \pm 0.08$  nm for the cluster galaxies observed in 1996. Thus the cluster galaxy distributions show no offset between the two runs, as is confirmed by a K-S test, and any systematic would therefore have preferentially to affect the field galaxies.

We first checked whether the stars used to remove atmospheric absorptions have had any effect on the measured CO EW values. However, all of the stars were drawn from a very small range of spectral types, with no chance of any intrinsic CO absorption. They were bright enough that the chance of misidentification is very slight, and in any case, no correlation was found between the derived CO EW and the star used. There are many cases where the same star was used for galaxies which were found to have CO EW values drawn from opposite extremes of the measured range, and conversely using different stars for a given galaxy spectrum was found to have no effect on derived EW values within the errors. Airmass differences between the galaxy and star observations were also found to have no measurable effect on the CO EWs.

We checked for wavelength calibration differences between the two runs, but no systematic difference was found. The CO EW definition adopted by PDW is, in any case, only weakly sensitive to wavelength errors, and any shift large enough to give the observed offset between the two field galaxy groups in Fig. 1 would have been immediately apparent in the spectra. The same argument also excludes redshift errors as the source of this effect, with shifts of  $\pm 400$  km s $^{-1}$  only changing the derived EW by  $\pm 0.1$  nm in the most extreme cases.

The instrument configuration was quite different between the two runs, and indeed a different detector array had been installed. The main consequences of this were a longer wavelength range for the 1996 run, giving a longer continuum baseline, and a somewhat coarser wavelength resolution for the 1994 observations. This gives rise to a number of possible effects on the derived CO values. One concerns the power-law fitting and extrapolation, which is better constrained for the more recent data, and the difference in spectral resolution could also potentially cause an effect due to rounding error in the wavelength range over which the equivalent width was calculated. To check for any systematic effects on the derived CO strengths, we re-reduced the more recent spectra, reducing the wavelength range and rebinning into coarser pixels in the wavelength direction, to match the wavelength range and resolution of the 1994 data. CO strengths were then derived from these simulated spectra, and were found to differ by up to 0.25 nm from values originally derived. In every case, most of the change was due to fitting the power-law continuum over a smaller wavelength range, as was demonstrated by producing spectra where the wavelength range and the resolution were changed individually. However, even the largest differences found by changing both wavelength range and resolution are much smaller (by a factor of at least 4) compared with the offset between the two field galaxy groups shown in Fig. 1.

Finally, the Galactic latitudes of the field galaxies were checked to explore if extinction effects might be significant. However, both the high-EW and low-EW groups have  $|b|$  distributions which

are approximately uniform over the range  $20^\circ$  and  $60^\circ$ , with no galaxies outside these limits.

Thus we have checked all the potential systematic effects of which we are aware, and none contributes significantly to the offset between the two groups of field galaxy CO strengths in Fig. 1. We therefore conclude that this represents a real difference between the galaxies, and continue now to discuss astrophysical explanations for this.

When selecting field galaxies for the 1994 run, we based our choice purely on information tabulated by Faber et al. (1989), checking only that ‘field’ galaxies were not members of major clusters. However, for the 1996 run, we selected field galaxies from highly isolated environments, thus maximising the environmental difference between field and cluster samples. Thus there is a strong correlation between degree of isolation and observing run, which we now propose explains the offset in field galaxy properties. Although these are all nominally field galaxies, there is in fact quite a wide range of environments sampled by these 19 galaxies, ranging from complete isolation up to membership of groups with  $\sim 10$  bright members. The criterion we adopt for complete isolation is that there be no companions within  $\sim 5$  magnitudes in apparent brightness, within a projected radius of 500 kpc. Of the 19 field galaxies, 6 meet this criterion (IC 5157, NGC 6020, NGC 6127, NGC 7391, NGC 7785 and ESO462–G015). At the other extreme, 4 galaxies are found in groups rich enough to have been identified by Huchra & Geller (1982) or Geller & Huchra (1983), who employed an algorithm based on position and redshift information only, to identify significant groupings in the CfA redshift survey and another magnitude-limited, all-sky sample. These galaxies are identified in Table 1. In addition, NGC 1600 is generally considered to lie at the center of a group of at least 10 members. The other 8 members of our field subset have at least one apparent companion but are fairly isolated, lying in groups with at most a few members.

It is interesting to note that all 6 completely isolated galaxies lie in the low–CO peak while the 5 galaxies in moderately rich groups lie in the high–CO peak in Fig. 1. The remaining ‘field’ galaxies, with a small number of apparent companions, are split between the two peaks. An interpretation of this result will be discussed in section 5.

It is also of interest to investigate the possible correlation of CO EW with environment for the cluster galaxies. However, Fig. 2 shows no correlation between CO EW and projected distance of galaxies from cluster centres.

#### 4 SPECTROSCOPIC PROPERTIES OF ELLIPTICALS

In this section, we briefly look at correlations between the spectroscopic CO EWs and other physical parameters of ellipticals in our sample.

A weak dependence is found between the CO EW and the metallicity of ellipticals, with the latter being measured by the  $Mg_2$  index (Fig. 3). There is the hint of a correlation in the expected sense, but this is formally only at the  $1-\sigma$  level. This is unsurprising given that previous studies have shown the CO index to be a poor metallicity indicator in old and metal-rich stellar populations. For example, Frogel et al. (1978) found no gradient in the photometric CO index with radius, even though galaxies have strong metallicity gradients as shown by optical indicators. There is a correlation between  $Mg_2$  and absolute B magnitude, in the sense that more luminous galaxies have higher metallicity (Fig. 4). However, this does not reflect in any measureable correlation between CO EW and absolute B magnitudes, as shown in Fig. 5, which also shows that the scatter in CO EW is constant with galaxy luminosity. Fig. 6 shows CO EW plotted against  $H\beta$  equivalent width, for the 19 galaxies in the present sample which were observed in the optical by Trager et al. (1998). Since  $H\beta$  is strong in stellar populations with relatively recent star formation, it is reassuring to

see a trend, however weak, in the expected sense in this plot, but the formal significance of the correlation is low due to the small number of objects for which data are available, and due to the different ages of populations probed by the two indicators.

Some of the individual galaxies have known peculiarities which might affect their star formation histories and hence the measured CO EWs. For example, NGC 1052 hosts a liner-type nucleus with broad H $\alpha$  emission and optical–near-IR line ratios inconsistent with stellar excitation (Alonso-Herrero et al. 1997), and is thus concluded to have a central nonstellar ionizing source. NGC 6051 is the radio source 4C+24.36 (Olsen 1970). NGC 6137 is identified as a head-tail radio source by Ekers (1978). NGC 6166, a multiple-nucleus cD galaxy in Abell 2199, is a strong radio source (3C338). Carollo et al. (1997) note that HST WFPC2 images of NGC 7626 show a warped, symmetrical dust lane crossing the centre, and this galaxy also has strong radio jets (Jenkins 1982). The compilation of radio surveys by Calvani, Fasano & Franceschini (1989) contains radio observations for 12 of the present sample; of these, 5 are detections (NGC 1052, NGC 1600, NGC 7385, NGC 7626 & NGC 7785) while the remainder (IC 5157, NGC 380, NGC 384, NGC 410, NGC 6020, NGC 7454 & NGC 7562) are all upper limits. Since any links between star formation and nuclear activity are highly uncertain at present, we make no comment on these data, other than to note that no strong correlation of radio properties with CO EW is evident.

## 5 DISCUSSION

The main issue confronted in this study is the effect of environment on the stellar population in elliptical galaxies (i.e. the epoch of star formation). Using the CO measurements for field and cluster ellipticals, we find no overall evidence for a stronger CO absorption feature in field galaxies compared to those in clusters, contrary to what was found in paper I. However, we find a clear difference between the CO strengths of ellipticals in small groups, with a few companions, and those which are truly isolated. Galaxies located in groups have CO EW values larger than either the isolated field subset, or than the cluster galaxies. Therefore, a simple monotonic correlation between star formation history and local galaxy number density seems untenable. This is the most important result from the present study.

However, it is unlikely to be a coincidence that the ellipticals appearing to contain young stars are preferentially located in environments most conducive to merging, due to the lower velocity dispersion of the groups compared to rich clusters, and indeed to merging with late-type companions, which are far more common in groups than rich clusters. Thus we propose, along with Ellis et al. (1997), that *all* ellipticals formed most of their stars at an early epoch, and those containing younger stars have acquired them recently through minor mergers with gas-rich galaxies. This is also suggested by Silva & Bothun (1998) in a study using near-infrared photometry of ellipticals which show signs of interaction/mergers. It is, however, likely that our spectroscopy, which only samples the central few arcsec, is more sensitive to such a component if the merging is strongly dissipative, with the accreted material rapidly sinking to the centre. Thus, our data should be more sensitive to nuclear starbursts than would be the global colours measured by Silva & Bothun (1998).

The observed offset between the isolated field subsample and the main peak of cluster galaxies in Fig. 1 is not a metallicity effect since they have similar mean  $M_{g_2}$  indices (which are measures of metallicity), corresponding to  $0.304 \pm 0.004$  mag. (for the ‘isolated’ ellipticals) and  $0.295 \pm 0.005$  mag. (for the cluster ellipticals). Therefore, given the weak correlation between  $M_{g_2}$  and CO EW (Fig. 2), the offset between isolated and cluster galaxies must have some other cause. However, there is a striking difference between the *range* of  $M_{g_2}$  indices for the different subsamples. The standard



deviation of the  $Mg_2$  indices for the isolated galaxy subsample is only 0.01 mag, c.f. 0.03 mag for the cluster galaxies and 0.04 mag for the group galaxies. While we must beware small number statistics (only 6 of the isolated galaxies have  $Mg_2$  values), this indicates that the isolated ellipticals form a very homogeneous group of galaxies, a point which is also indicated by the extreme narrowness of the corresponding peak in CO EW values shown in Fig. 1. Conversely, the large range in  $Mg_2$  for the group galaxies is easily understood if these are prone to significant merging and accretion activity.

There have been several studies claiming to have found intermediate-age populations in field galaxies (e.g. Bica & Alloin 1987, Bower et al. 1990, Schweizer & Seitzer 1992, Rose 1994). It is therefore of interest to see whether these are consistent with the interpretation presented above. Bica & Alloin (1987) find 5 individual galaxies which show clear evidence of intermediate-age or young stellar populations. Of these, 4 (NGC 2865, NGC 5018, NGC 5061 & NGC 5102) are listed by Faber et al. (1989) as being members of groups with group velocity dispersions between 120 and 430 km s<sup>-1</sup>. The only exception is NGC 4382, an interacting S0 on the outskirts of the Virgo cluster. Thus, all the 5 galaxies are located in environments conducive to merging activity. The same is true for the ellipticals studied by Rose et al. (1994), where all of the field ellipticals lie in the outer regions of the Virgo cluster, or in groups identified by Faber et al. (1989), with group velocity dispersions between 65 and 210 km s<sup>-1</sup>. Since the majority of ellipticals lie in groups or clusters, this can hardly be taken as a striking confirmation of our model, but it is encouraging that there are no discrepant objects in these two independent studies.

Further observations are clearly required to test our present interpretation. CO spectroscopy should be obtained for field galaxies claimed by other studies (e.g. Bica & Alloin 1987; Rose et al. 1994) to have undergone recent star formation, and for the apparent post-merger objects of Silva & Bothun (1998). It is also important to extend the present sample of very isolated galaxies to confirm the very homogeneous old populations we have found in the present paper. Our present interpretation in terms of recent merging predicts a correlation between CO absorption strength and the velocity dispersion of the group or cluster in which the galaxy resides; it will be of interest to see whether such a correlation is confirmed by future observations of galaxies in a range of environments from the core of the Coma cluster to the field.

In order to calibrate the observed differences in CO strengths in terms of starburst ages and strengths, reliable evolutionary synthesis models are required. This is an area which is yet to be fully developed in terms of near-IR spectroscopic parameters, but some preliminary work has been done. Buzzoni (1995) tabulates CO indices for simulated stellar populations with ages between 4 and 15 Gyr, and in general predicts strengths similar to those in the isolated field galaxies in the present sample. For example, taking a Salpeter IMF and solar metallicities, the CO indices predicted by Buzzoni (1995) convert to equivalent widths of 2.4–3.0 nm, using the conversion formulae given by Doyon et al. (1994) and PDW. This agreement is encouraging, but it should be noted that these models cannot explain the strength of CO absorption observed in the ‘group’ ellipticals. Even if there is an overall offset between the model predictions and observations, it is interesting to note that Buzzoni et al. (1995) find only ~10% change in CO absorption strength between 4 Gyr and 15 Gyr populations (the extremes in the modelled ages), for any reasonable IMF and metallicity. The ~30% difference observed between the ‘isolated’ and ‘group’ galaxies thus requires either a population of stars significantly younger than 4 Gyr in the ‘group’ galaxies, a combination of age and metallicity effects (but see the discussion earlier in this section) or may point to an additional stellar component which is not accurately reproduced in the existing models. This latter is quite possible, given the complexity of evolution of giant and supergiant stars.

## 6 CONCLUSIONS

Contrary to the main conclusion of paper I, we do not find evidence for an overall offset in CO absorption strength, between field and cluster ellipticals. However, there is a bimodal distribution in this parameter for field galaxies only, with the two distributions directly correlated with the degree of isolation of galaxies. Specifically, very isolated ellipticals appear to form a very homogeneous population, with no sign of recent star formation and a very small range of metallicity as revealed by their  $Mg_2$  absorption feature. On the other hand, ellipticals in groups frequently show evidence for intermediate-age stellar populations and have a wide range in metallicity. Ellipticals in rich clusters have intermediate properties in both parameters.

We interpret the observed differences in terms of recent minor mergers, which are most likely to occur in the moderate density environment of small groups consisting of only a few members. Dissipative mergers with gas-rich galaxies could then introduce a significant population of younger stars to the central regions of galaxies in these groups, giving the stronger CO absorptions we find. If this is the case, then our data are consistent with ellipticals in all environments being essentially old, in agreement with other recent studies.

Further work is clearly needed to extend the size of the isolated and group samples, to test further whether the somewhat *a posteriori* division of the field galaxies is actually justified. In addition, the whole area of near-IR spectroscopy of galaxies is ripe for detailed stellar spectral synthesis modelling, so that data of the type we present here can be fully understood.

## ACKNOWLEDGMENTS

We thank the anonymous referee for several useful recommendations which significantly improved the content and presentation of this paper. PJ thanks Doug Burke for useful suggestions. This research has made use of the NASA/IPAC Extragalactic Database (NED) which is operated by the Jet Propulsion Laboratory, California Institute of Technology, under contract with the National Aeronautics and Space Administration. The United Kingdom Infrared Telescope is operated by the Joint Astronomy Centre on behalf of the U.K. Particle Physics and Astronomy Research Council.

## REFERENCES

- Allen, C. W., 1976, *Astrophysical Quantities (3rd ed.)*, Athlone Press, London
- Alonso-Herrero A., Rieke M. J., Rieke G. H., Ruiz M., 1997, ApJ, 482, 747
- Bica E., Alloin D., 1987, A&A, 181, 270
- Bower R. G., Ellis R. S., Rose J. A., Sharples R. M., 1990, AJ, 99, 530
- Bower R. G., Lucey J. R., Ellis R. S., 1992, MNRAS, 254, 601
- Bruzual G., 1983, ApJ, 273, 105
- Butcher H. R., Oemler A., 1985, ApJS, 65, 665
- Buzzoni A., 1995, ApJS, 98, 69
- Calvani M., Fasano G., Franceschini A., 1989, AJ, 97, 1319
- Carollo C. M., Franx M., Illingworth G. D., Forbes D. A., 1997, ApJ, 481, 710
- de Carvalho R. R., Djorgovski S., 1992, ApJ, 389, L49
- Djorgovski, S., Davis, M., 1987, ApJ., 313, 59
- Doyon R., Joseph R. D., Wright G. S., 1994, ApJ, 421, 101
- Dressler, A., Lynden-Bell, D., Burstein, D., Davies, R.L., Faber, S.M., Terlevich, R.J., Wegner, G., 1987, ApJ, 313, 42
- Ekers R. D., 1978, A&A, 69, 253
- Ellis R. S., Smail I., Dressler A., Couch W. J., Oemler A., Butcher H., Sharples R.M., 1997, ApJ, 483, 582
- Faber S. M., Wegner G., Burstein D., Davies R. L., Dressler A., Lynden-Bell D., Terlevich R. J., 1989, ApJS, 69, 763.
- Fogel J. A., Persson S. E., Aaronson M., Matthews K., 1978, ApJ, 220, 75
- Geller M. J., Huchra J. P., 1983, ApJS, 52, 61 (GH)
- Gonzalez J. J., 1993, Ph.D. thesis, Univ. California, Santa Cruz
- Guzmán R., Lucey J. R., 1993, MNRAS, 263, 47
- Huchra J. P., Geller M. J., 1982, ApJ, 257, 423 (HG)
- Jenkins C. R., 1982, MNRAS, 200, 705
- Kauffmann G., 1996, MNRAS, 281, 487
- Kleinmann S. G., Hall D. N. B., 1986, ApJS, 62, 501
- Larson R. B., Tinsley B. M., Caldwell C. N., 1980, ApJ, 237, 692
- Lucey J. R., Guzmán R., Steel J., Carter D., 1997, MNRAS, 287, 899
- Mobasher B., James P. A., 1996, MNRAS, 280, 895 (paper I)
- O'Connell R. W., 1980, ApJ, 236, 430
- Olsen E. T., 1970, AJ, 75, 764
- Origlia L., Moorwood A. F. M., Oliva E., 1993, A&A, 280, 536
- Puxley P. J., Doyon R., Ward M. J., 1997, ApJ, 476, 120 (PDW)
- Rose J. A., Bower R. G., Caldwell N., Ellis R. S., Sharples R. M., Teague P., 1994, AJ, 108, 2054
- Schweizer F., Seitzer P., 1992, AJ, 104, 1039
- Silva D. R., Bothun G. D., 1998, AJ, 116, 85
- Tinsley B.M., Gunn J.E., 1976, ApJ, 203, 52
- Trager S.C., Worthey G., Faber S.M., Burstein D., Gonzalez J., 1998, ApJS, 116, 1

## Figure Captions

**Figure 1.** A histogram showing the distribution of CO EW values for cluster (solid line) and field (dashed line & shading) ellipticals.

**Figure 2.** CO EW as a function of projected distance from the cluster centre, for 30 ellipticals in rich clusters.

**Figure 3.** CO EW as a function of the metallicity index  $Mg_2$  for the 44 elliptical galaxies. Plotted symbols are the same as for Fig. 2.

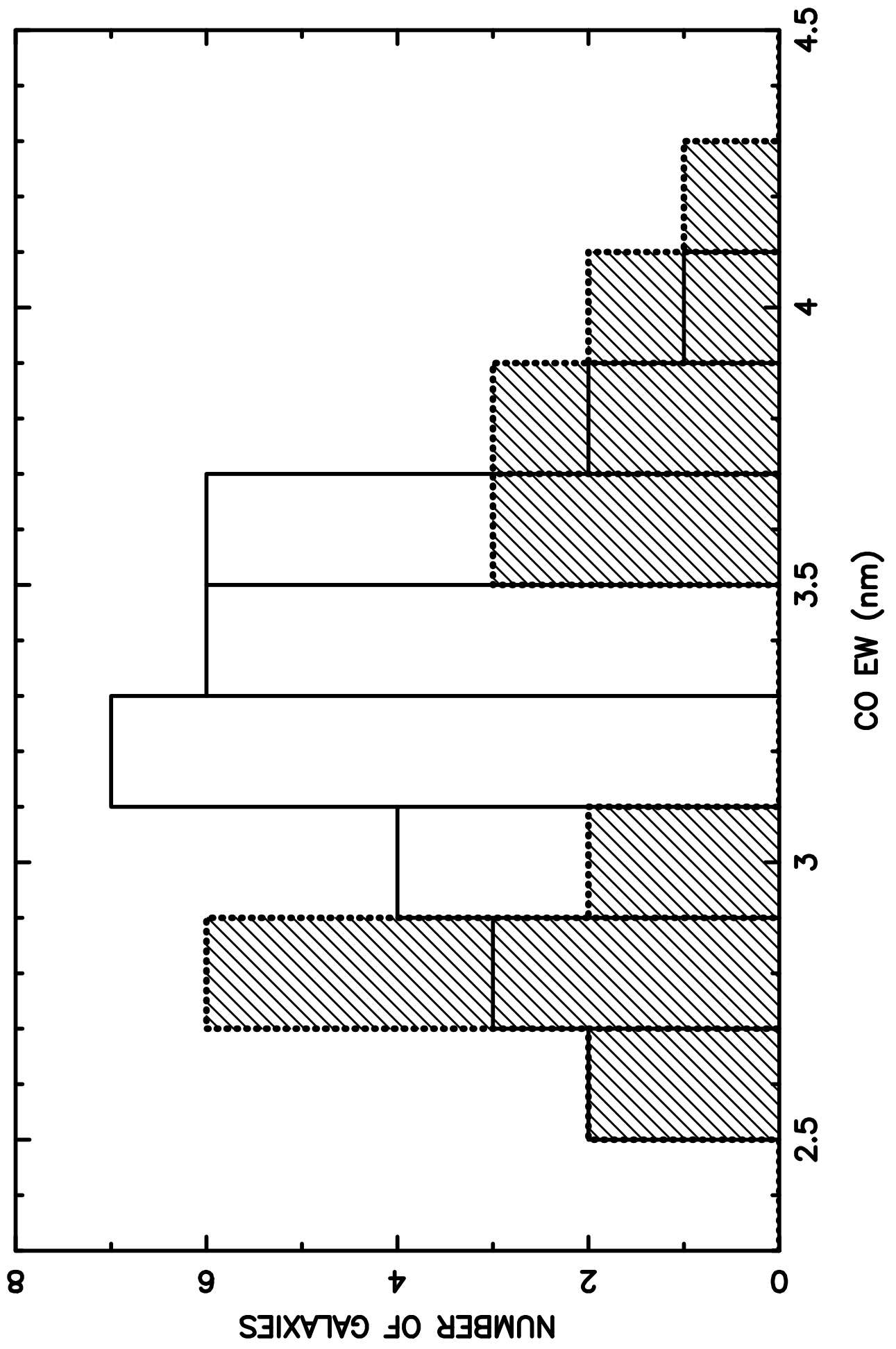
**Figure 4.** Metallicity index  $Mg_2$  as a function of total B-band absolute magnitude for 44 elliptical galaxies. Plotted symbols are the same as for Fig. 2.

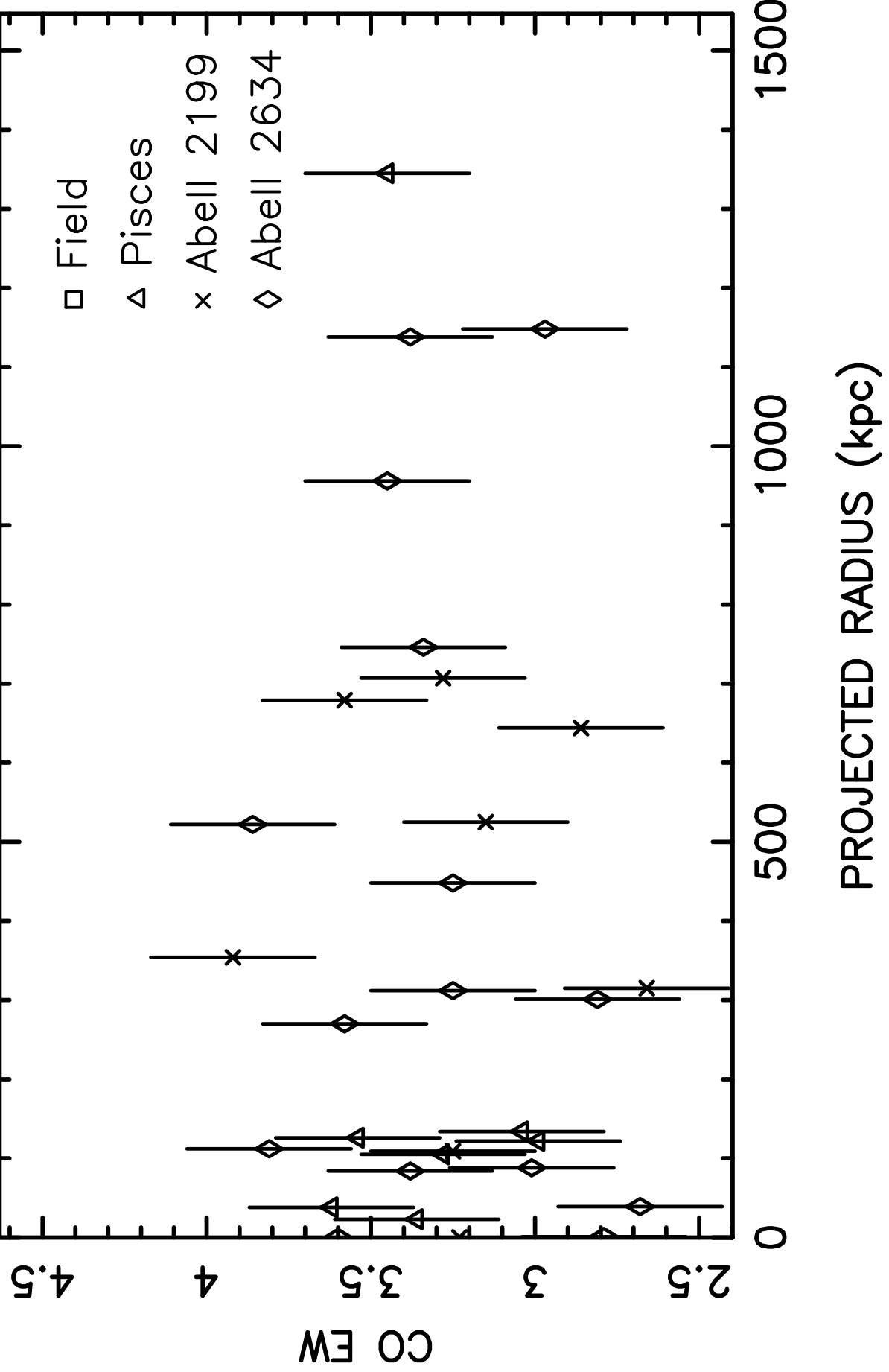
**Figure 5.** CO EW as a function of total B-band absolute magnitude for 50 elliptical galaxies. Plotted symbols are the same as for Fig. 2.

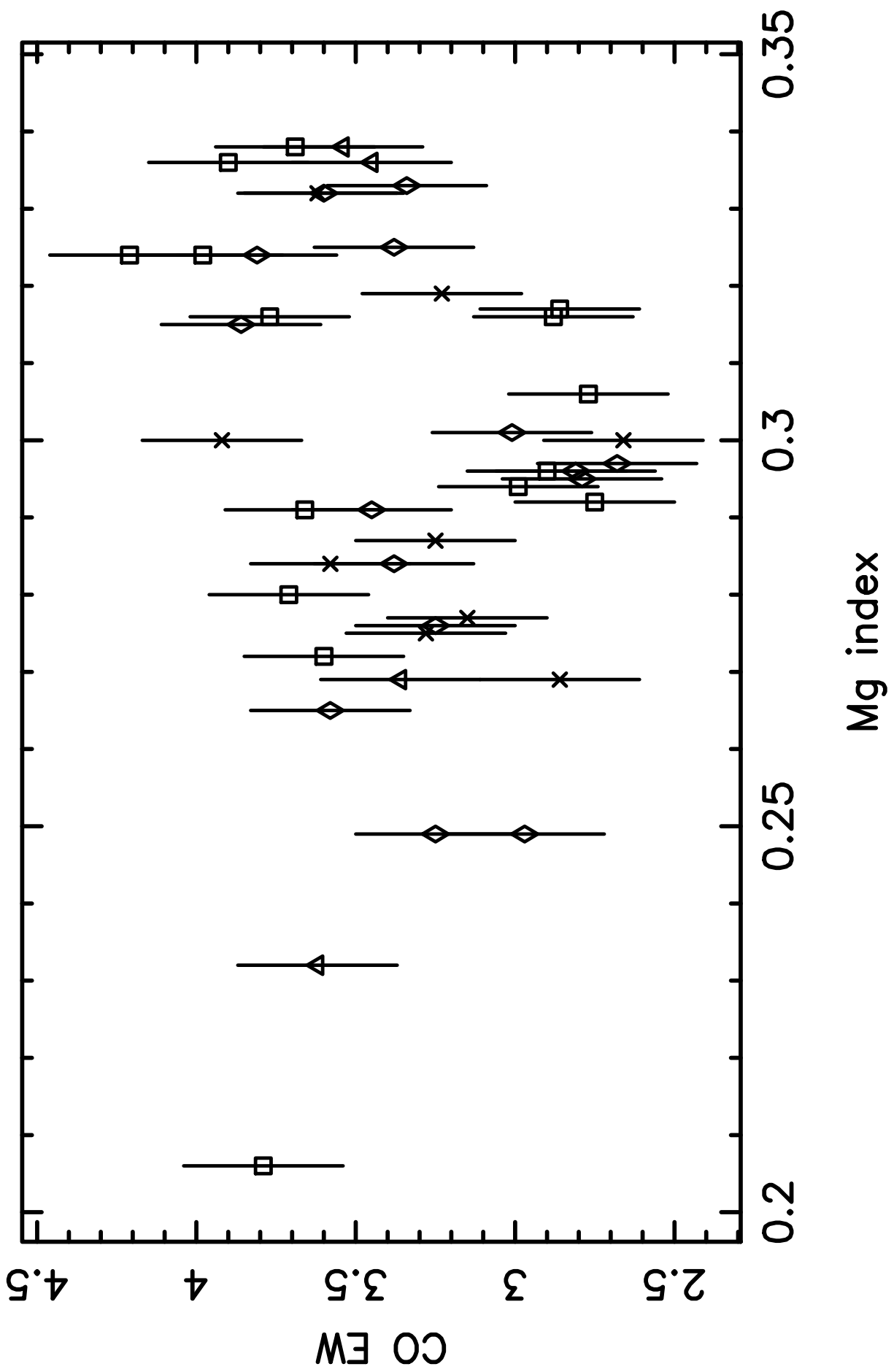
**Figure 6.** CO EW as a function of  $H\beta$  EW for 19 elliptical galaxies. Plotted symbols are the same as for Fig. 2.

**Table 1**

Name	V	CO <sub>sp</sub>	EW	H $\beta$	M <sub>B</sub>	$\sigma$	Mg <sub>2</sub>	Cluster
IC 5157	4443	0.231	2.59	-	-20.72	-	-	Isol
NGC 1052	1474	0.246	3.77	-	-20.12	2.313	0.316	HG44
NGC 1600	4718	0.285	4.21	1.30	-22.16	2.506	0.324	N1600 gr
NGC 6020	4397	0.241	2.77	1.70	-20.15	2.296	0.306	Isol
NGC 6051	9588	0.274	3.69	2.03	-21.58	2.386	0.338	-
NGC 6127	4609	0.238	2.88	1.33	-21.02	2.355	0.316	Isol
NGC 6137	9306	0.248	2.99	0.63	-22.07	2.496	0.294	-
NGC 6577	5205	0.227	2.86	-	-20.51	-	-	-
NGC 6702	4712	0.259	3.60	2.43	-20.95	2.259	0.272	-
NGC 6703	2365	0.257	3.71	1.74	-20.52	2.233	0.280	-
NGC 7385	7809	0.250	3.98	1.29	-21.83	2.414	0.324	-
NGC 7391	3045	0.221	2.86	1.74	-20.08	2.436	0.317	Isol
NGC 7454	1991	0.275	3.79	2.11	-19.42	2.050	0.206	GH163
NGC 7562	3636	0.275	3.66	1.74	-21.05	2.385	0.291	GH166
NGC 7626	3423	0.289	3.90	1.27	-21.24	2.369	0.336	GH166
NGC 7680	5177	0.227	2.79	-	-21.27	-	-	-
NGC 7785	3849	0.231	2.90	1.66	-21.14	2.464	0.296	Isol
E462-G015	5827	0.234	2.75	-	-21.91	2.467	0.292	Isol
E468-G013	6890	0.230	2.59	-	-20.48	-	-	-
NGC 375	6011	0.210	3.28	-	-19.60	-	-	Pisces
NGC 380	4384	0.267	3.54	0.75	-20.46	2.443	0.338	Pisces
NGC 382	5217	0.259	3.36	1.06	-20.25	2.185	0.269	Pisces
NGC 384	4398	0.213	2.99	-	-20.02	-	-	Pisces
NGC 386	5555	0.249	3.62	-	-19.49	1.785	0.232	Pisces
NGC 388	5114	0.197	3.04	-	-19.29	-	-	Pisces
NGC 410	5296	0.248	3.45	2.32	-22.01	2.507	0.336	Pisces
NGC 6158	8914	0.233	3.15	2.03	-20.70	2.280	0.277	A2199
NGC 6166	9414	0.277	3.23	0.44	-22.67	2.475	0.319	A2199
NGC 6173	8771	0.244	3.62	-	-22.17	2.417	0.332	A2197
A2199-103	9400	0.275	3.92	-	-19.32	2.252	0.300	A2199
A2199-105	8677	0.245	2.66	-	-19.27	2.243	0.300	A2199
A2199-121	8780	0.288	3.25	-	-20.15	2.240	0.287	A2199
A2199-BO5	8704	0.277	3.58	-	-20.50	2.312	0.284	A2199
A2199-BO8	9280	0.242	2.86	-	-20.24	2.146	0.269	A2199
A2199-BO26	9136	0.248	3.28	-	-20.06	2.310	0.275	A2199
NGC 7720	9130	0.245	3.60	0.71	-22.33	2.520	0.332	A2634
A2634-BO5	9345	0.257	3.86	-	-20.69	2.450	0.315	A2634
A2634-BO4	9981	0.229	2.81	-	-21.09	2.326	0.296	A2634
NGC 7728	9498	0.244	3.34	-	-21.71	2.519	0.333	A2634
UGC 12733	11850	0.225	2.97	-	-21.54	2.422	0.249	A2634
A2634-102	9251	0.266	3.58	-	-20.14	2.291	0.265	A2634
A2634-121	9586	0.209	3.38	-	-18.52	2.263	0.284	A2634
A2634-124	9846	0.217	2.68	-	-21.42	2.273	0.297	A2634
A2634-134	9297	0.246	3.01	-	-20.04	2.345	0.301	A2634
A2634-139	9520	0.245	3.81	-	-20.20	2.335	0.324	A2634
A2634-1222	8088	0.229	2.79	-	-20.12	2.312	0.295	A2634
A2634-1482	9347	0.252	3.25	-	-21.22	2.383	0.276	A2634
A2634-BO9	9970	0.253	3.45	-	-21.54	2.317	0.291	A2634

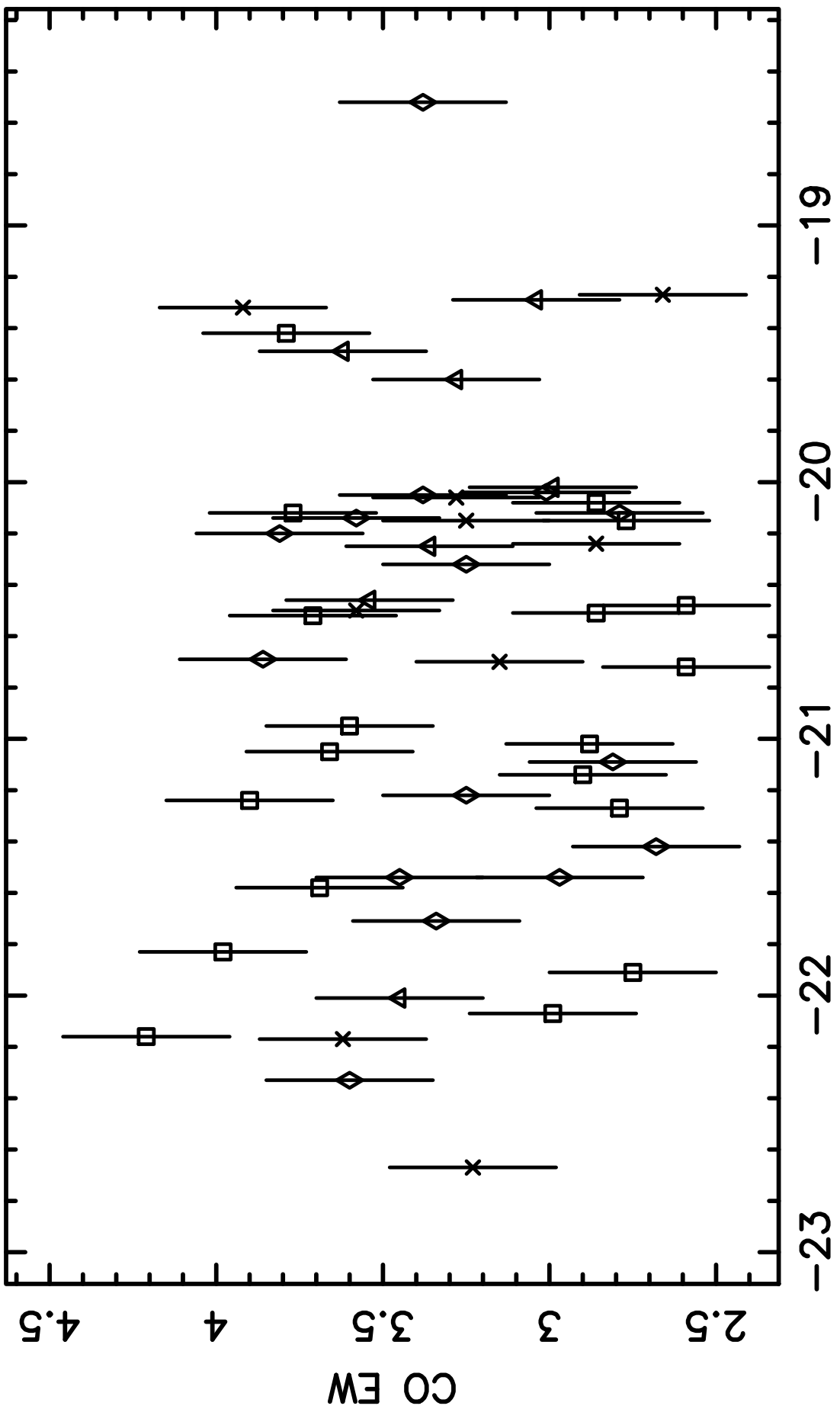












B absolute magnitude

